Purifying hydrogen from dilute hydrogen-natural gas mixtures using HT-PEM electrochemical hydrogen pumps

Karthik Arunagiri[1], John M. Turssline[1], and Christopher G. Arges[1,⊥]*

[1] Department of Chemical Engineering, The Pennsylvania State University, University Park, PA, 16802, USA
*Corresponding author: chris.arges@psu.edu
[⊥] Current address: Argonne National Laboratory, 9700, S Cass Ave, Lemont, IL 60439, USA, carges@anl.gov

Abstract

Reducing the cost of hydrogen transport is an important priority for proliferation of clean hydrogen to decarbonize various sectors of industry and heavy-duty vehicle transportation. Pipeline transport of gases is the lowest cost delivery method for gases over long distances, but there are only a few pipeline networks dedicated to hydrogen. It is possible to alleviate clean hydrogen transportation costs by delivering it via existing natural gas pipeline infrastructures. This strategy, however, necessitates dilution of hydrogen by blending it with natural gas as the hydrogen can embrittle existing pipeline materials. An electrochemical hydrogen pump (EHP) is a separation platform capable of de-blending hydrogen from natural gas mixtures at end use locations because many applications require purified hydrogen. In this work, we deploy high-temperature polymer electrolyte membrane (HT-PEM) EHPs to purify hydrogen from dilute hydrogen-natural gas mixtures (i.e., 5 to 20 vol% hydrogen). The HT-PEM EHP uses an ion-pair HT-PEM with perfluorosulfonic acid-phosphonic acid ionomer blends as electrode binders. Interestingly, we observe that activation overpotentials govern HT-PEM EHP polarization when feeding dilute hydrogen mixtures. We ascribe this observation to interfacial mass transfer resistance of hydrogen through the ionomer binder to the electrocatalyst surface resulting in a lower surface concentration

of hydrogen and a lower exchange current density. Pressurizing the anode to 1.76 bar_{abs} ameliorates the interfacial mass transfer resistance and enabled us to achieve an EHP limiting current of 1.4 A cm^{-2} with a 10 vol% of hydrogen in natural gas feed. This configuration also pressurized the hydrogen at the cathode to 2.51 bar_{abs}. The HT-PEM EHP showed a small degradation rate, 44 μV h^{-1}, during a 100-hour durability test purifying 10 vol% hydrogen-natural gas feed mixtures to 99.3 vol% hydrogen.

Introduction

Hydrogen usage is anticipated to grow at a rapid pace as it is an important chemical for decarbonizing industry, assisting with seasonal energy storage, and powering fuel cell engines used in heavy-duty vehicle transportation.[1] The first Earthshot™ announced by the U.S. Department of Energy aims to reduce costs for producing clean hydrogen to $1 per kg within a decade.[2] However, green hydrogen production costs in 2023 hover around $4 per kg.[3]

One overlooked consideration in the adoption of clean hydrogen is the costs associated with hydrogen storage and distribution – which are on par with today's green hydrogen production cost.[4] Alleviating hydrogen distribution costs can be achieved via pipeline transport, but building out new pipeline is a large upfront investment and a timely endeavor – especially since permitting is required to build pipeline over large distances. It has been proposed to use the existing natural gas pipeline infrastructure for transporting hydrogen because there is about 3 million miles of natural gas distribution pipelines in the United States[5] carrying 27.6 trillion cubic feet (Tcf)[6] of natural gas. Other common methods to store hydrogen include storage using sorbents[7], metal hydrides[8], and liquid organic hydrogen carriers (LOHCs)[9]. However, storage of hydrogen using these technologies is limited by either large-scale use (material saturation) or converting hydrogen

to another form, such as ammonia, methanol, or methylcyclohexane, which requires additional processing.[10]

There are several challenges in storing and transporting hydrogen in the natural gas pipeline. The biggest concerns are hydrogen leakage from the pipeline and embrittlement of natural gas pipeline materials.[111] Coating the pipeline with polyethylene has been proposed to ameliorate the embrittlement problem[12], however, the effect of hydrogen on polyethylene is not fully understood at high pressures and exposure over long time.[13] Diluting the hydrogen can mitigate embrittlement, but end users of the transported hydrogen require high purity for their operations. It has been proposed to purify hydrogen from dilute hydrogen-natural gas mixtures at end point uses using an electrochemical hydrogen pump (EHP). This technology is electrified and contains no moving parts and can co-currently pressurize the purified hydrogen at the cathode[14]. The latter step reduces the energy burden on a downstream compressor. EHPs were first developed by General Electric[15] and their variant used perfluorosulfonic acid (PFSA) proton exchange membranes. However, PFSA membranes require humidification for proton transfer; and the natural gas pipeline does not control humidity in the gas mixture. There have only been a few demonstrations of separating hydrogen from methane or natural gas mixtures with EHPs – many of of which use low temperature proton exchange membrane (LT-PEM).[16-19] Nonetheless, the previous works neither purified hydrogen from a dilute hydrogen-natural gas mixtures (less than 10% as needed in natural gas pipeline) while also achieving a current density value of 1 A cm^{-2}. The latter attribute is necessary to reduce the EHP system size and captial cost. Alternative separation units for purifying hydrogen include pressure swing and temperature swing adsorption[20] units and palladium membranes[21], but these unit operations place a bigger burden on downstream compressors because they cannot perform simultaneous separation and compression like an EHP.

Figure 1a shows a conceptual design for storing and distributing hydrogen in natural gas pipeline and purifying it via an EHP. **Figure 1b** illustrates the experimental high-temperature polymer electrolyte membrane (HT-PEM) EHP setup used in this work to purify hydrogen from diluted hydrogen-natural gas mixtures. This Figure shows the mass flow controllers to mix hydrogen and natural gas to generate feed compositions for the anode and it also shows the on-line micro gas chromatography (GC) system used to measure the cathode effluent composition. **Figure 1c** conveys the ion-pair HT-PEM and electrode binder material chemistries used in the EHP.

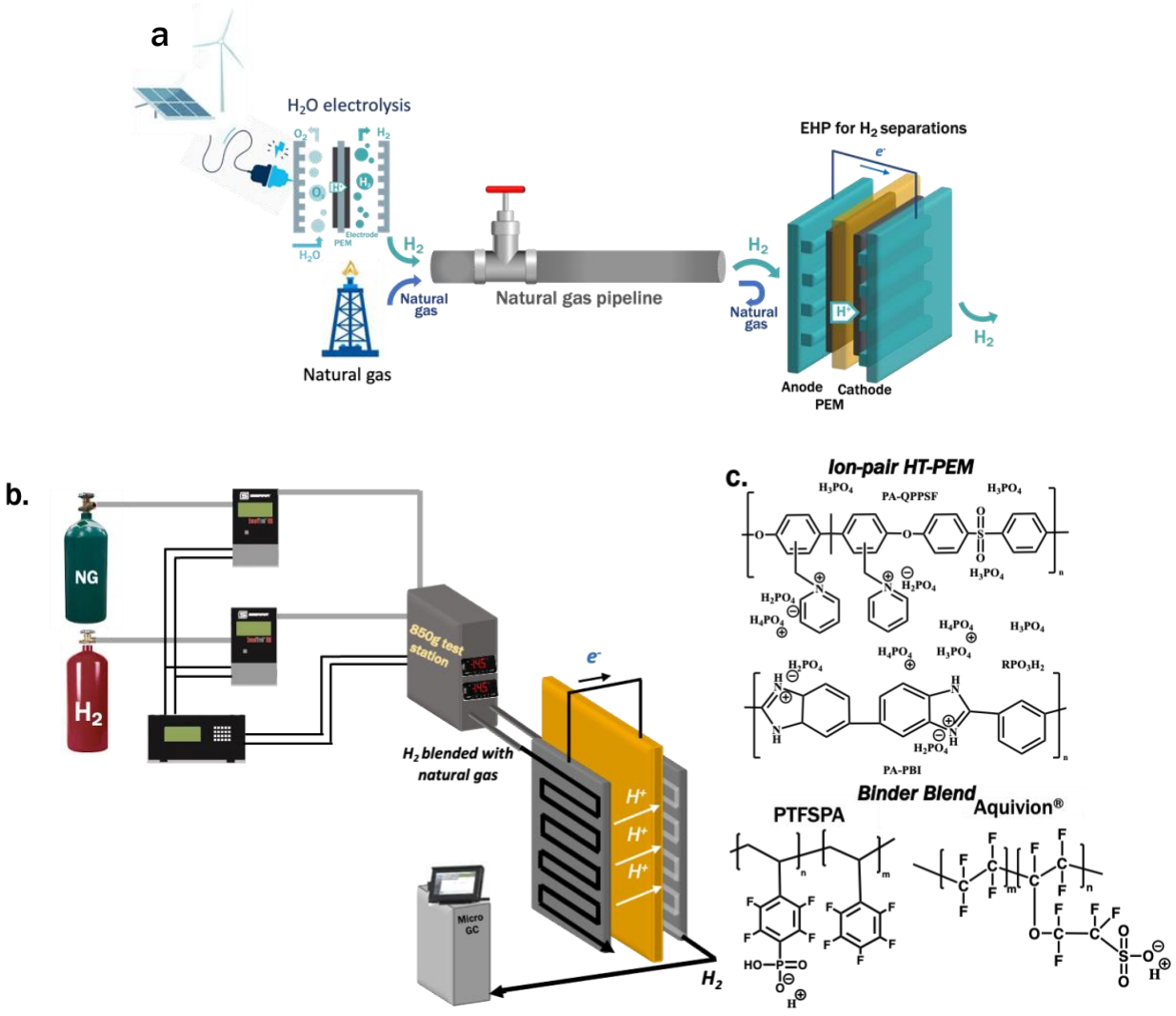

Figure 1. (a) An illustrated concept conveying distribution of hydrogen in the natural gas pipeline by blending it with natural gas and purifying it at end use points using an electrochemical hydrogen pump (EHP). (b) A high-temperature polymer electrolyte membrane (HT-PEM) EHP experimental setup with hydrogen mixed with natural gas to feed into the anode of the EHP. The on-line micro GC measures the cathode's effluent composition. (c) The chemical structures of the ion-pair HT PEM and electrode binders used in the EHP for this work.

The emergence of ion-pair HT-PEMs[22, 23] with electrode binders consisting of phosphonic acid ionomer[24] and perfluorosulfonic ionomer blends[25] has led to remarkable achievements in HT-PEM fuel cells and EHP performance. HT-PEM systems with these materials can operate over a wide temperature range, such as room temperature to 200 °C[26], without external humidification to facilitate proton conduction. Because the hydrogen-natural gas mixtures will not contain water, or will have small amounts of water vapor present, it is important to leverage a separation platform that does not require humidification of the feed gas stream. In our previous work[27], we demonsrated an EHP that achieved 5.1 A cm^{-2} at 0.4 V when using a pure hydrogen feed and electrode binders consisting of poly(pentafluorostyrene-*co*-tetrafluorostyrene phosphonic acid) (i.e., PTFSPA) blended with Aquivion® (a short-side chain perfluorosulfonic acid (PFSA) ionomer). This study also used an ion-pair HT-PEM. Furthermore, this work showed that electrode binder ionomers consisting of PTFSPA blended with Aquivion® gave the best EHP performance and proton conductivity when compared to other phosphonic acid ionomers (such as poly(vinyl phosphonic acid) and poly(vinyl benzyl phosphonic acid) blended with Aquivion® or PTFSPA blended with Nafion™. The addition of PFSA to phosphonic acid ionomers in electrode layers not only promoted proton conductivity, but also enhanced electrode kinetics and hydrogen gas diffusivity.

In this work, we purified hydrogen from dilute hydrogen (5, 10, and 20 vol%)-natural gas feed mixtures to 99.3 vol% using an EHP containing an ion-pair HT-PEM and phosphonic acid

ionomer-PFSA ionomer blends as electrode binders. We chose this hydrogen concentration in natural gas range because it represents that values that will be acceptable for storing and distributing hydrogen in the natural gas pipeline. **Table S1** lists the volume composition of natural gas components before blending with hydrogen. The methane content in the natural gas used in this work is typical of the natural gas found in the field - which ranges from 87% to 97%.[19, 28] Using electrochemical impedance spectroscopy (EIS), we unexpectedly observe that charge-transfer kinetics with different hydrogen feed concentrations has the biggest impact on cell polarization. It was initially posited that diluting the hydrogen content further would cause large increases in the electrode diffusion resistance; however, the changes in charge-transfer kinetic resistances were much greater than the changes in diffusion resistances. We ascribe these observations to interfacial hydrogen transport resistances from the gas phase through the ionomer to the electrocatalyst surface. The interfacial mass transfer resistances were reduced by pressurizing the anode to 1.76 bar_{abs} allowing the EHP to operate at 1.4 A cm^{-2} (limiting current) with a 10 vol% hydrogen-natural gas mixtures while purifying the hydrogen to > 99.2 vol%. We also show that the EHP is stable for 100 hours at 200 °C for purifying hydrogen from 10 vol% hydrogen-natural gas mixtures with no performance loss.

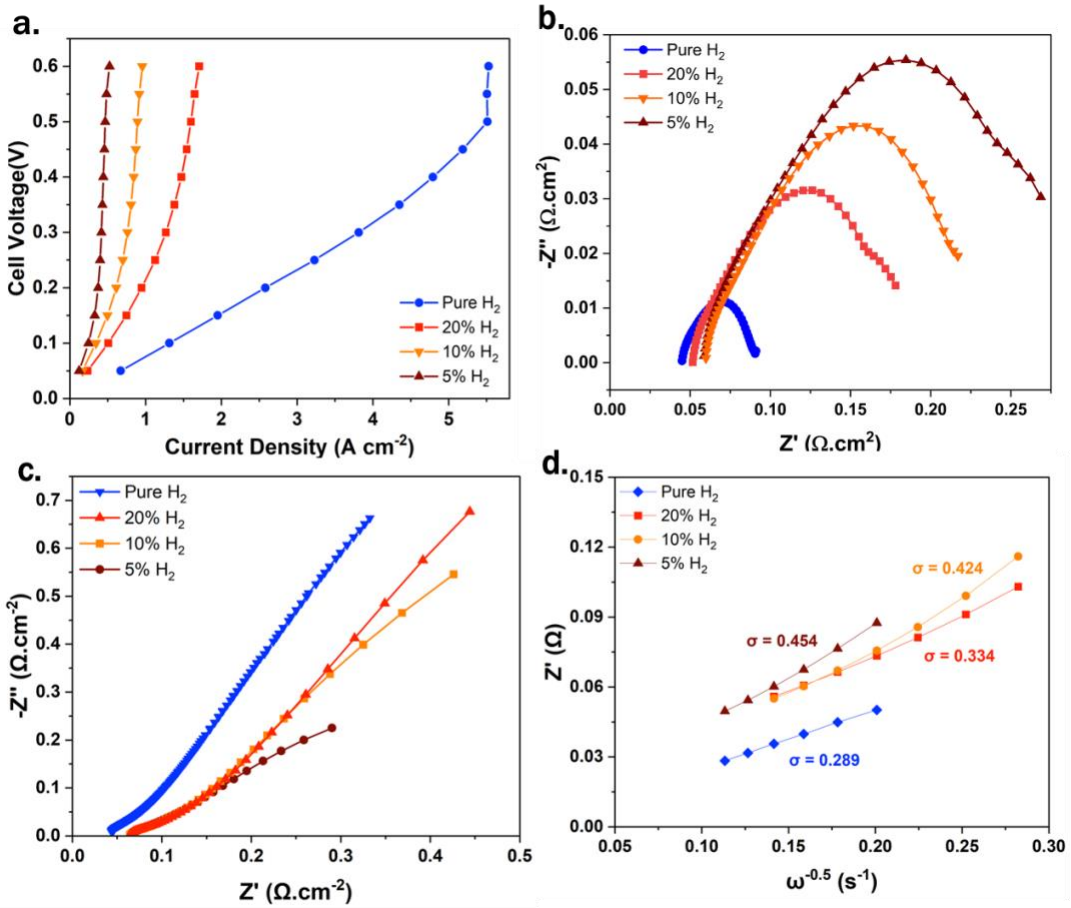

Figure 2. (a) EHP polarization curves for the different H_2-NG mixtures and pure H_2 at 200 °C; (b) EIS with DC bias of 0.05V at T = 200 °C with H_2-NG mixtures and pure H_2; (c) EIS with DC bias of 0.55V at T = 200 °C with H_2-NG mixtures and pure H_2; (d) Warburg plot showing the diffusion resistance (σ) calculated from the Nyquist plots in (c).

Figure 2a presents the polarization curves of the EHP at 200 °C with an ion-pair HT-PEM and phosphonic acid ionomer-PFSA ionomer blend electrode binders with different dilute hydrogen-natural gas (H_2-NG) feed mixtures to the anode and a control case of pure hydrogen to the anode. No back pressure was applied to the anode or the cathode in these experiments. The pure hydrogen polarization curve data was reported in our previous work.[27] The polarization curves at different cell temperatures, 120 °C and 160 °C, are provided in **Figures S2a** and **S3a**. The polarization data in **Figures 2a, S3a,** and **S4a** demonstrate that the cell polarization increases when feeding more dilute hydrogen-natural gas mixtures. We anticipated this effect for two

reasons: i) the Nernst equation predicts that the minimum cell voltage needed for purifying the hydrogen increases when starting with a more dilute feed on the anode side while maintaining approximately the same purity and partial pressure of hydrogen on the cathode side and ii) we anticipated greater diffusion resistance within the porous anode when feeding more dilute hydrogen. The purity of the hydrogen exiting the cathode of the EHP was analyzed using micro-GC and the results of the cathode gas effluent composition is shown in Table 1. The purity was analyzed at two different current densities: one at a lower current density and other near the limiting current. The purity of the hydrogen emanating from the cathode was ≥ 99.3vol% at 160 and 200 °C. At 120 °C, the purity of the hydrogen from the cathode was 99.039 to 99.096 vol%.

Table 1. Cathode effluent composition from EHP experiments with a 5 vol% H_2 and 95 vol% NG

EHP condition	**200°C**		**160°C**		**120°C**	
Current Density	**0.25 A cm^{-2}**	**0.48 A cm^{-2}**	**0.1 A cm^{-2}**	**0.4 A cm^{-2}**	**0.1 A cm^{-2}**	**0.3 A cm^{-2}**
H_2	99.371	99.356	99.742	99.669	99.096	99.039
CH_4	0.578	0.539	0.112	0.179	0.872	0.81
N_2	0.019	0.02	0.111	0.118	0.008	0.117
CO_2	0.003	0.023	0.022	0.024	0.016	0.024
C_2H_6	-	0.006	0.01	0.008	0.005	0.008

EIS was deployed to determine the ohmic, electrode kinetics, and electrode diffusion resistances within the HT-PEM EHP when using different hydrogen-natural gas feed mixtures. These experiments were performed with different background cell voltages to examine a kinetically controlled case and a mass-transfer controlled case. **Figure 2b** presents the Nyquist plot with a 0.05 V cell voltage in the background. **Figures S3b** and **S4b** give the Nyquist plots for measurements performed at 120 and 160 °C, respectively, at the same cell voltage. The Nyquist plots in **Figures 2b, S3b,** and **S4b** feature semi-circles with no tails in the low-frequency regime further supporting the cell is not mass transfer limited. When changing the background voltage to

0.55 V, the Nyquist plots (**Figures 2c, S3c** and **S4b**) do not show a distinct semi-circle. Rather, they display a large tail indicating a diffusion-controlled process. To determine the diffusion related resistances with the different feed gases to the anode, Warburg plots (**Figures 2d**, **S3d**, and **S4d**) were constructed by plotting Z_{real} versus the inverse square root of the angular frequency in the low frequency regime from the data in **Figures 2c, S3c,** and **S4c**. The slope of the lines in the traces of **Figures 2d**, **S3d**, and **S4d** correspond to the diffusion related resistances.

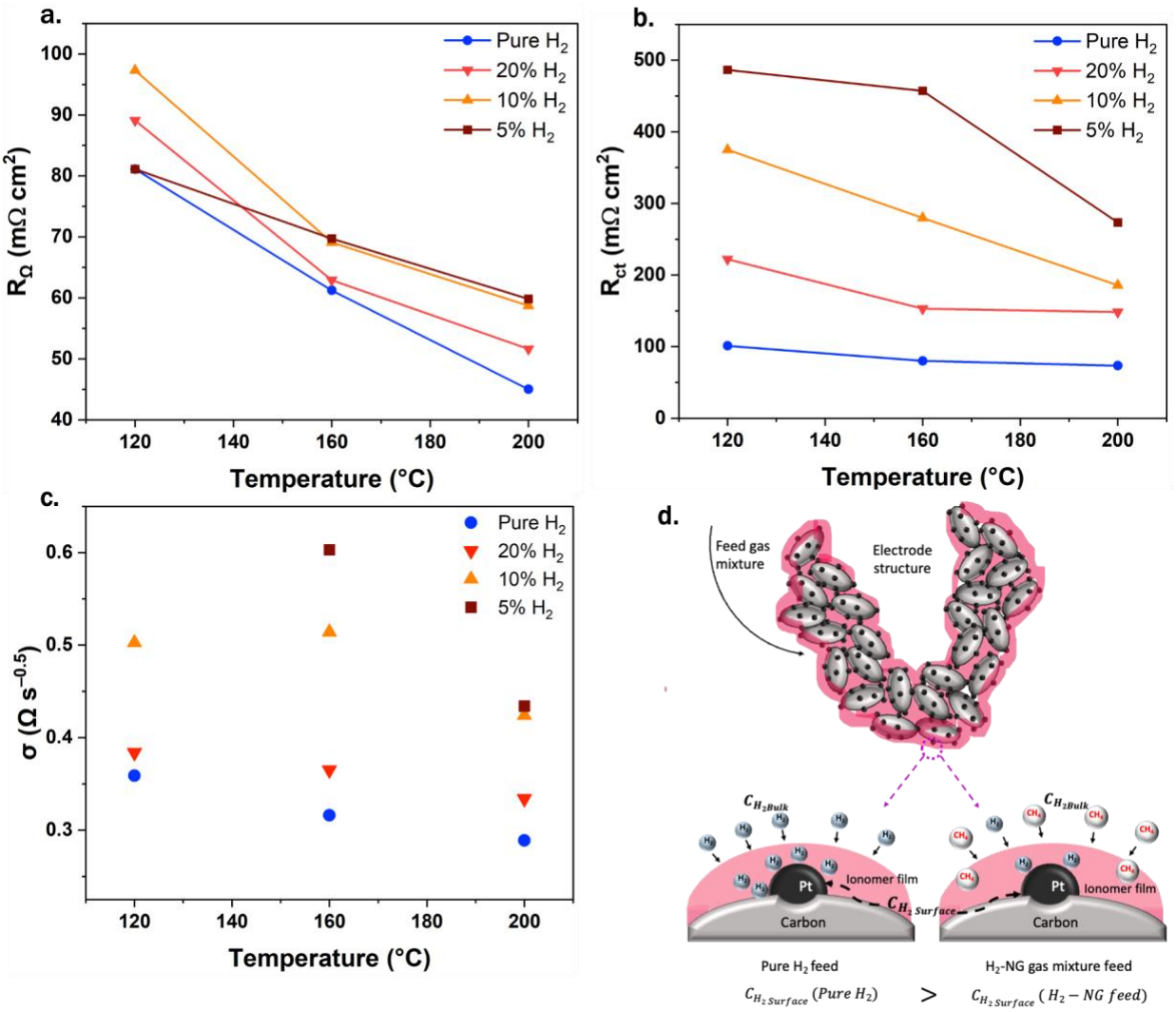

Figure 3. Extracted resistance values from the cell using EIS as a function of temperature and H_2 feed concertation: (a) ohmic (R_Ω), (b) charge-transfer (R_{ct}), and (c) diffusion related resistances; (d) Electrode structure showing the effect of using H2-NG gas mixtures on H_2 concentration at Pt catalyst surface along with various interfacial resistances for H_2 transport.

Figures 3a, 3b, and **3c** present the ohmic resistance (R_Ω), charge-transfer resistance (R_{ct}), and diffusion resistance (σ) values determined from EIS for each feed gas mixture concentration and cell temperature evaluated. Increasing the cell temperature reduced each of the said resistances resulting in the reduced polarization (**Figs 2a, S3a,** and **S4a**). Notably, the diffusion resistance for the extreme case of comparing pure hydrogen to 5 vol% hydrogen in natural gas went up by 1.5x to 2x at 200 °C and 160 °C, respectively, while the charge-transfer resistance went up 3x at 200 °C and about 5x at temperatures 120 °C and 160 °C. The ohmic resistance showed the least change when switching from pure hydrogen to dilute hydrogen feed mixtures: 1.2x to 1.4x across the temperature range.

We originally posited that the largest changes in cell resistance would hail from diffusion related resistance when reducing the hydrogen concentration in the anode feed. Concentration polarization is largely governed by the concentration of the reactant. However, **Figure 3** clearly demonstrates that charge-transfer resistance values increased the most when lowering the hydrogen concentration in the feed. Charge-transfer resistances are largely ascribed to reaction kinetics and are inversely commensurate to the exchange current density of the electrodes[29] when the cell or working electrode is at low overpotentials. The exchange current density evaluated from the charge transfer resistance are shown in **Figure S4** in the SI. Because > 99% hydrogen is being produced at the cathode, the anode will have the largest contributor to the charge-transfer resistance. The exchange current density is often described as a proxy for the reaction rate coefficient, but the derivation of the Butler-Volmer equation clearly shows that the exchange current density is commensurate to the reaction rate coefficient multiplied by the surface concentration of the reactant. We surmise that the large increases in charge-transfer resistance with

lower concentrations of hydrogen in the natural gas mixture hails from interfacial mass transfer resistances from the gas phase in the porous electrode through the ionomer to the electrocatalyst surface (**Figure 3d**). The lower concentration of hydrogen in the gas phase gives a smaller concentration gradient between gas in the porous electrode to the electrocatalyst surface. This leads to a smaller surface concentration of hydrogen at the ionomer-electrocatalyst interface as shown in **Figure 3d** and a lower exchange current density value and an increase in charge-transfer kinetics.

Finally, it is worth pointing out that the ohmic resistance ($R\Omega$) underwent a slight increase (in all cases but one) when diluting the hydrogen concentration in the feed gas. We originally anticipated no changes in the ohmic resistance of the cell when changing the composition of the feed gas. We surmise that the hydrogen concentration in the gas feed will alter the proton activity in the anode affecting the anode proton conductivity and ohmic resistance. This motivates future work to examine these ionomer material's proton conductivity as a function of hydrogen content in the gas feed.

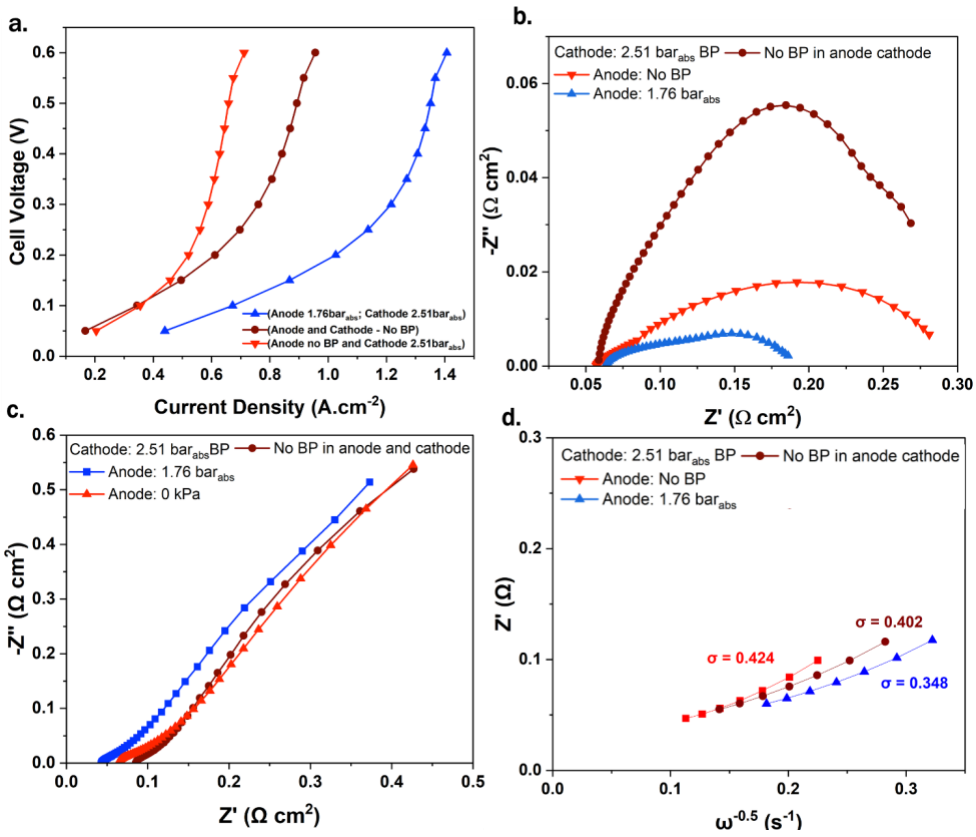

Figure 4. (a) EHP polarization curves of 10 vol% H_2-NG mixture with no back pressure applied, back pressure applied to the cathode only, and back pressure applied to the anode and cathode (1.76 bar_{abs} and 2.51 bar_{abs}, respectively); (b) EIS with a back ground voltage of 0.05 V for the said experiments with different back pressures; (c) EIS with a background voltage of 0.55V for the said experiments; (d) Warburg plot showing the diffusion resistances (σ) when applying backpressure and no back pressure on the cell.

Because we hypothesized that interfacial mass transfer resistance values affect charge-transfer kinetics in the anode, we performed EHP experiments with back pressure on the anode and compared it against control experiments with no back pressure on the cell and back pressure on the cathode only. The feed gas and cell temperature remained constant in these experiments: 10 vol% hydrogen-natural gas and T = 200 °C. Many EHP demonstrations pressurize the cathode as downstream use of the purified or recovered hydrogen needs to be pressurized; otherwise, the energy use on the downstream mechanical compressor is very high (i.e., the energy use on the downstream mechanical pressure can be reduced by partially pressurizing the purified hydrogen

emanating from the cathode). Our current hardware prevents us from applying back pressure greater than 2.51 bar_{abs}. Furthermore, a partial compression of the hydrogen emanating from the cathode reduces the energy burden on the downstream compressor. **Figure 4a** shows the EHP polarization for the control cases of no back pressure applied on the anode and cathode and 2.51 bar_{abs} on the cathode only (conventional use of EHP). This Figure also presents the polarization data when applying 1.761 bar_{abs} on the anode and 2.51 bar_{abs} on the cathode. Comparison of the two control cases shows that increasing cathode back pressure with no back pressure on the anode increases cell polarization. Pressuring the anode while also pressurizing the cathode to a higher value (which was done to avoid a Galvanic cell[30]) reduced cell polarization and increased the limiting current density.

EIS was performed with two different voltages in the background to assess changes in the cell resistance values when changing the back pressure on the anode and/or cathode. **Figure 4b** shows that pressurizing the anode reduces the charge-transfer resistance by 40% when compared to the two cases. Interestingly, the imaginary values for the control case of no back pressure on both electrodes were 2x to 3x larger near the apex than back pressure on the cathode. However, the real part of the traces where it almost crosses the x-axis a second time is the same (i.e., similar charge-transfer resistances values). The origins the change in the imaginary part of the semi-circles for the two control cases will be part of a future study looking at the impedance spectra more rigorously. The imaginary values can be related to the capacitive behavior of the cell.

Figure 4c presents the Nyquist plots for the EHP with different back pressure values on the cell with a background voltage of 0.55 V. This voltage was selected because it is at the limiting current of the cell – signaling that the anode is mass transfer limited. The Warburg plots given in **Figure 4d** were constructed from the data in **Figure 4c** to assess diffusion resistances in the

electrode. Diffusion resistance values were reduced 13 to 18% when applying back pressure on the anode when compared against the two control cases. The results from **Figure 4** demonstrates that applying anode back pressure has a profound impact on reducing charge-transfer resistances (40% reduction) while a smaller effect on diffusion resistances in the anode (13 to 18% reduction). This provides evidence that interfacial mass transfer resistance of hydrogen through the ionomer binder governs EHP polarization when purifying hydrogen from dilute natural gas mixtures.

The interfacial mass transfer resistance arises from poor permeability of hydrogen across the high-temperature ionomers used in this study. This large interfacial resistance does not occur with hydrogen in PFSA ionomers used in low-temperature systems that are well-hydrated. Permeability is the product of the gas solubility in the material multiplied by its diffusion coefficient (assuming the solution-diffusion model). Hydrogen diffusivity and solubility values become larger in PFSA ionomers when increasing hydration[31]. The HT-PEM EHP and feed gases do not contain water. Hence, we posit that the non-hydrated ionomer blend used in this work may have poor hydrogen solubility and diffusivity. This motivates future work to study the said properties in high-temperature ionomers. Another potential reason for the large interfacial resistances observed could hail from phosphoric acid in the electrode layers. In HT-PEM fuel cells, phosphoric acid migrates from the membrane host to the porous electrodes[32]. Ion-pair HT-PEMs significantly curb the amount of acid leaching when compared to the conventional PBI variant. However, it is worth pointing out that a fuel cell generates water at the cathode and that water within the cathode can supplant acid from the membrane host to the electrode. The EHP is not generating water and has no water in the gas feed. Therefore, there could be less phosphoric acid redistribution in EHPs.

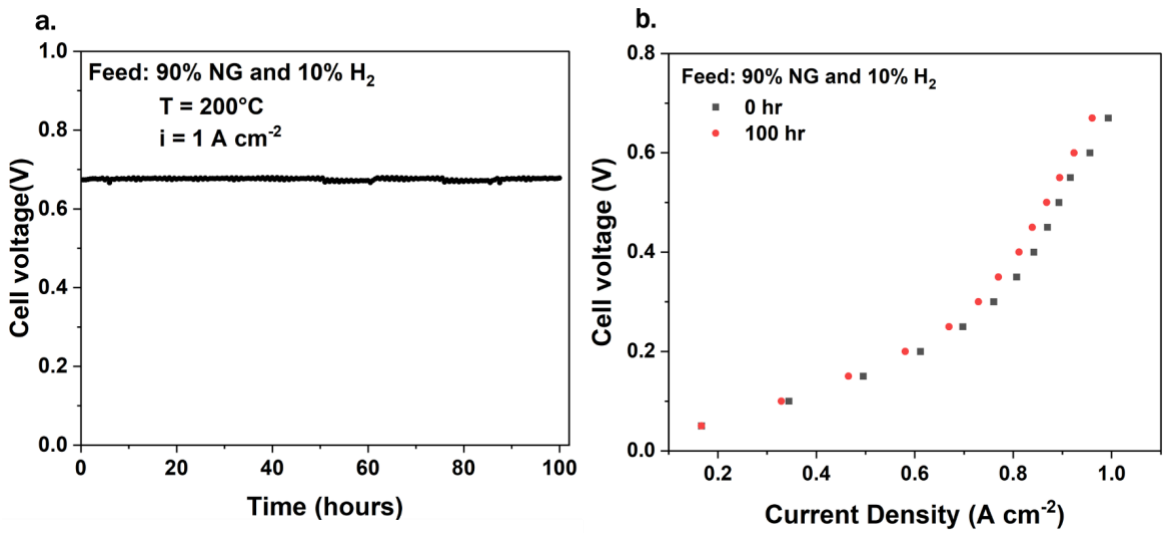

Figure 5. (a) HT-PEM EHP stability test at 200 °C and a constant current density of 1A cm^{-2} with 10% H_2-90%NG mixture feed to the anode. (b) HT-PEM EHP polarization at 200 °C with 10% H_2-90% NG mixture before and after the 100-hour stability test.

The final experiments examined the durability of the EHP for purifying hydrogen from 10 vol%-natural gas feeds. The durability occurred at 200 °C at a constant current density of 1A cm^{-2} for 100 hours. **Figure 5a** shows the cell voltage versus time, while **Figure 5b** gives the polarization curve before and after the test. The cell voltage degradation rate was 44 µV h^{-1}. The changes in polarization curve from beginning of life to after the durability test was about 3.5% reduction in current density for a given cell voltage. The hydrogen purity emanating from the cathode was >99.5 vol% at the 64 hour and > 99.4 vol% at 99 hour time points during the durability test. Future experiments will explore thicker membranes or a multistage EHP setup to generate ultra-pure hydrogen (>99.99%). Overall, an HT-PEM EHP with an ion-pair membrane and PTFSPA-Aquivion® as electrode binders is effective for purifying dilute hydrogen from natural gas mixtures over a long period of time.

In summary, a HT-PEM EHP was used to purify hydrogen from dilute hydrogen-natural gas mixtures at 5 vol%, 10 vol%, and 20 vol% in the feed mixtures. This platform is envisioned to provide end users purified hydrogen when delivered as a dilute gas in the natural gas pipeline. For the three different feed mixtures, the EHP purified the hydrogen from the gas mixtures to > 99.09 vol%. By comparing the cell polarization and various resistances extracted from EIS, we unexpectedly observed that reducing the hydrogen concentration in the feed substantially increases the charge-transfer resistance. This effect was attributed to interfacial mass transfer resistance of the hydrogen across the ionomer binder to the electrocatalyst surface. The interfacial mass transfer resistance was curbed by applying back pressure to the anode, and this led to an EHP with a large limiting current of 1.4 A cm^{-2} when feeding 10 vol% hydrogen in natural gas. The EHP showed a small degradation rate (44 µV h^{-1}) over a 100 hour durability test at T = 200 °C when purifying a 10 vol% hydrogen-natural gas mixture to greater 99.4 vol% hydrogen.

Author Contributions

K.A. performed all synthesis of the materials and experiments with materials; J.M.T. prepared all the HT-PEM membrane used in this study. K.A., and C.G.A. wrote the manuscript. All authors contributed to the data analysis and editing of the manuscript.

Declaration of Interests

A patent application was filed on this work by The Penn State Research Foundation.

Acknowledgments

This material is based upon work supported by the U.S. National Science Foundation Award Number 2143056. We acknowledge the usage of Penn State's shared user facilities for access to NMR and ellipsometry equipment. Special acknowledgment to Greg Payne from the Agilent Technologies, Inc. for helping us setup the Micro GC and assisting with data analysis.

Supporting Information

The Supporting Information contains characterization data of the PTFSPA ionomer (NMR spectra, IEC, and thin film conductivity), procedure for gas composition analysis by an on-line micro-GC analyzer, EHP polarization results at 120 °C and 160 °C, and a comparison of EHP performance data in the literature versus this work.

References

1. Bararzadeh Ledari, M.; Khajehpour, H.; Akbarnavasi, H.; Edalati, S., Greening steel industry by hydrogen: Lessons learned for the developing world. *International Journal of Hydrogen Energy* **2023,** *48* (94), 36623-36649.
2. Pivovar, B. S.; Ruth, M. F.; Myers, D. J.; Dinh, H. N., Hydrogen: Targeting $1/kg in 1 Decade. *The Electrochemical Society Interface* **2021,** *30* (4), 61.

3. Saini, A. Outlook for green and blue hydrogen market **2023**. https://www.gep.com/blog/strategy/Green-and-blue-hydrogen-current-levelized-cost-of-production-and-outlook.
4. Mahajan, D.; Tan, K.; Venkatesh, T.; Kileti, P.; Clayton, C. R., Hydrogen Blending in Gas Pipeline Networks ;A Review. *Energies* **2022,** *15* (10).
5. Skelton, M. Natural Gas Distribution US DOE EERE, **2018**. https://afdc.energy.gov/fuels/natural_gas_distribution.html.
6. Wagner, N. Natural gas explained U.S. Energy Information Administration, **2022**. https://www.eia.gov/energyexplained/natural-gas/natural-gas-pipelines.php.
7. Rimza, T.; Saha, S.; Dhand, C.; Dwivedi, N.; Patel, S. S.; Singh, S.; Kumar, P., Carbon-Based Sorbents for Hydrogen Storage: Challenges and Sustainability at Operating Conditions for Renewable Energy. *ChemSusChem* **2022,** *15* (11), e202200281.
8. Klopčič, N.; Grimmer, I.; Winkler, F.; Sartory, M.; Trattner, A., A review on metal hydride materials for hydrogen storage. *Journal of Energy Storage* **2023,** *72*, 108456.
9. Chu, C.; Wu, K.; Luo, B.; Cao, Q.; Zhang, H., Hydrogen storage by liquid organic hydrogen carriers: Catalyst, renewable carrier, and technology – A review. *Carbon Resources Conversion* **2023,** *6* (4), 334-351.
10. Zhang, C.; Shao, Y.; Shen, W.; Li, H.; Nan, Z.; Dong, M.; Bian, J.; Cao, X., Key Technologies of Pure Hydrogen and Hydrogen-Mixed Natural Gas Pipeline Transportation. *ACS Omega* **2023,** *8* (22), 19212-19222.
11. Kappes, M. A.; Perez, T., Hydrogen blending in existing natural gas transmission pipelines: a review of hydrogen embrittlement, governing codes, and life prediction methods. **2023,** *41* (3), 319-347.
12. Lei, Y.; Hosseini, E.; Liu, L.; Scholes, C. A.; Kentish, S. E., Internal polymeric coating materials for preventing pipeline hydrogen embrittlement and a theoretical model of hydrogen diffusion through coated steel. *International Journal of Hydrogen Energy* **2022,** *47* (73), 31409-31419.
13. Kevin Topolski, E. P. R., Burcin Cakir Erdener, Chris W. San Marchi, Joseph A. Ronevich, Lisa Fring, Kevin Simmons, Omar Jose Guerra Fernandez, Bri-Mathias Hodge, and Mark Chung. Hydrogen Blending into Natural Gas Pipeline Infrastructure: Review of the State of Technology **2022**.
14. Marciuš, D.; Kovač, A.; Firak, M., Electrochemical hydrogen compressor: Recent progress and challenges. *International Journal of Hydrogen Energy* **2022,** *47* (57), 24179-24193.
15. Maget, H. J. R. Process for gas purification. 07/29/1964, **1970**.
16. Ibeh, B.; Gardner, C.; Ternan, M., Separation of hydrogen from a hydrogen/methane mixture using a PEM fuel cell. *International Journal of Hydrogen Energy* **2007,** *32* (7), 908-914.
17. Wu, X.; He, G.; Yu, L.; Li, X., Electrochemical Hydrogen Pump with SPEEK/CrPSSA Semi-Interpenetrating Polymer Network Proton Exchange Membrane for H2/CO2 Separation. *ACS Sustainable Chemistry & Engineering* **2014,** *2* (1), 75-79.
18. Onda, K.; Araki, T.; Ichihara, K.; Nagahama, M., Treatment of low concentration hydrogen by electrochemical pump or proton exchange membrane fuel cell. *Journal of Power Sources* **2009,** *188* (1), 1-7.
19. Jackson, C.; Smith, G.; Kucernak, A. R., Deblending and purification of hydrogen from natural gas mixtures using the electrochemical hydrogen pump. *International Journal of Hydrogen Energy* **2024,** *52*, 816-826.
20. Relvas, F.; Whitley, R. D.; Silva, C.; Mendes, A., Single-Stage Pressure Swing Adsorption for Producing Fuel Cell Grade Hydrogen. *Industrial & Engineering Chemistry Research* **2018,** *57* (14), 5106-5118.
21. Rahimpour, M. R.; Samimi, F.; Babapoor, A.; Tohidian, T.; Mohebi, S., Palladium membranes applications in reaction systems for hydrogen separation and purification: A review. *Chemical Engineering and Processing: Process Intensification* **2017,** *121*, 24-49.
22. Kim, Y. S.; Lee, K.-S.; Purdy, G. M.; Choe, Y.-K.; Fujimoto, C.; Han, J.; Bae, C., A New Class of Fuel Cells Based on Ion Pair-Coordinated Proton Exchange Membranes. *ECS Meeting Abstracts* **2017,** *MA2017-02* (34), 1470.

23. Venugopalan, G.; Chang, K.; Nijoka, J.; Livingston, S.; Geise, G. M.; Arges, C. G., Stable and Highly Conductive Polycation–Polybenzimidazole Membrane Blends for Intermediate Temperature Polymer Electrolyte Membrane Fuel Cells. *ACS Applied Energy Materials* **2020,** *3* (1), 573-585.
24. Atanasov, V.; Lee, A. S.; Park, E. J.; Maurya, S.; Baca, E. D.; Fujimoto, C.; Hibbs, M.; Matanovic, I.; Kerres, J.; Kim, Y. S., Synergistically integrated phosphonated poly(pentafluorostyrene) for fuel cells. *Nature Materials* **2021,** *20* (3), 370-377.
25. Lim, K. H.; Lee, A. S.; Atanasov, V.; Kerres, J.; Park, E. J.; Adhikari, S.; Maurya, S.; Manriquez, L. D.; Jung, J.; Fujimoto, C.; Matanovic, I.; Jankovic, J.; Hu, Z.; Jia, H.; Kim, Y. S., Protonated phosphonic acid electrodes for high power heavy-duty vehicle fuel cells. *Nature Energy* **2022,** *7* (3), 248-259.
26. Chaichi, A.; Venugopalan, G.; Devireddy, R.; Arges, C.; Gartia, M. R., A Solid-State and Flexible Supercapacitor That Operates across a Wide Temperature Range. *ACS Applied Energy Materials* **2020,** *3* (6), 5693-5704.
27. Arunagiri, K.; Wong, A. J.-W.; Briceno-Mena, L.; Elsayed, H. M. G. H.; Romagnoli, J. A.; Janik, M. J.; Arges, C. G., Deconvoluting charge-transfer, mass transfer, and ohmic resistances in phosphonic acid–sulfonic acid ionomer binders used in electrochemical hydrogen pumps. *Energy & Environmental Science* **2023,** *16* (12), 5916-5932.
28. Nayebossadri, S.; Speight, J. D.; Book, D., Hydrogen separation from blended natural gas and hydrogen by Pd-based membranes. *International Journal of Hydrogen Energy* **2019,** *44* (55), 29092-29099.
29. Horvai, G., Relationship between charge transfer resistance and exchange current density of ion transfer at the interface of two immiscible electrolyte solutions. *Electroanalysis* **1991,** *3* (7), 673-675.
30. Huang, F.; Pingitore, A. T.; Campbell, T.; Knight, A.; Johnson, D.; Johnson, L. G.; Benicewicz, B. C., A Thermoelectrochemical Converter Using High-Temperature Polybenzimidazole (PBI) Membranes for Harvesting Heat Energy. *ACS Applied Energy Materials* **2020,** *3* (1), 614-624.
31. Takeuchi, K.; Kuo, A.-T.; Hirai, T.; Miyajima, T.; Urata, S.; Terazono, S.; Okazaki, S.; Shinoda, W., Hydrogen Permeation in Hydrated Perfluorosulfonic Acid Polymer Membranes: Effect of Polymer Crystallinity and Equivalent Weight. *The Journal of Physical Chemistry C* **2019,** *123* (33), 20628-20638.
32. Lim, K. H.; Matanovic, I.; Maurya, S.; Kim, Y.; De Castro, E. S.; Jang, J.-H.; Park, H.; Kim, Y. S., High Temperature Polymer Electrolyte Membrane Fuel Cells with High Phosphoric Acid Retention. *ACS Energy Letters* **2023,** *8* (1), 529-536.